Available online at www.sciencedirect.com

ScienceDirect

Energy Procedia 8 (2011) 147–152

Energy Procedia

SiliconPV: 17-20 April 2011, Freiburg, Germany

Determination of the Collection Diffusion Length by Electroluminescence Imaging

Carsten Schinke[a,*], David Hinken[a], Karsten Bothe[a], Christian Ulzhöfer[a], Ashley Milsted[a], Jan Schmidt[a,b], Rolf Brendel[a,b]

[a]*Institute for Solar Energy Research Hamelin, Am Ohrberg 1, 31860 Emmerthal, Germany*
[b]*Institute of Solid-State Physics, University of Hannover, Appelstrasse 2, 30167 Hannover, Germany*

Abstract

The electroluminescence emission of crystalline silicon solar cells at near-bandgap wavelengths is investigated. We show that the intensity of the emitted luminescence at near-bandgap wavelengths is directly proportional to the collection diffusion length L_c which is a measure of bulk and rear surface recombination properties and determines the short circuit current of a solar cell illuminated with light of near-bandgap wavelengths. We provide experimental evidence for the determination of L_c by carrying out electroluminescence measurements on a set of 15 specially prepared monocrystalline silicon solar cells with different thicknesses. Moreover, we demonstrate and discuss the applicability of the proposed method to obtain images of the collection diffusion length L_c of multicrystalline silicon solar cells. The values determined by electroluminescence imaging coincide with values obtained from spectrally resolved quantum efficiency measurements with a relative accuracy of 13 %.

Keywords: electroluminescence imaging; collection diffusion length

1. Introduction

Spectrally resolved measurements of the quantum efficiency allow for a comprehensive analysis of solar cells with respect to recombination properties of the bulk and the rear surface. The evaluation of such measurements at near-infrared wavelengths (typically between 600 and 900 nm) enables the determination of the product of the effective diffusion length L_{eff} and the absorption length of light $L_\alpha = \alpha^{-1}$ [1]. Here α denotes the absorption coefficient. The effective diffusion length L_{eff} is a function of the bulk diffusion length L_b and the rear surface recombination velocity S_r. However, the association of a

* Corresponding author: Tel. (+49) 5151 / 999-632; fax (+49) 5151 / 999-400
E-mail address c.schinke@isfh.de

1876–6102 © 2011 Published by Elsevier Ltd. Selection and/or peer-review under responsibility of SiliconPV 2011.
Open access under CC BY-NC-ND license. doi:10.1016/j.egypro.2011.06.116

value of L_{eff} with a pair of L_b and S_r values is not unique. Thus, bulk and rear surface recombination effects cannot be clearly distinguished. To overcome this limitation, Basore introduced a method for separating bulk and rear surface recombination effects [1]. His approach is based on an extended analysis of spectrally resolved internal quantum efficiency (IQE) measurements carried out at near-infrared *and* near-bandgap wavelengths. At near-bandgap wavelengths, the collection diffusion length L_c [2] can be extracted. L_c is also a function of the bulk diffusion length L_b and the rear surface recombination velocity S_r. While L_{eff} determines the base saturation current density, L_c determines the short circuit current of a solar cell which is illuminated with light of near-bandgap wavelengths. Figure 1 visualizes the dependencies of L_{eff} and L_c on L_b and S_r. Following Basore, measuring both L_c and L_{eff} allows to reduce the parameter range of L_b and S_r [1, 3]. In this publication, however, we will focus on the determination of L_c.

IQE measurements usually determine global properties of the solar cell. Since solar cells are large area devices, local measurements provide more information. It is thus desirable to measure both L_{eff} and L_c with appropriate accuracy and spatial resolution. IQE measurements featuring a complete wavelength scan combined with high lateral resolution would, however, result in an unacceptably long measurement duration. As an alternative, the local determination of L_{eff} is possible using spectrally resolved light beam induced current (SR-LBIC) [4] measurements. This scanning method determines the quantum efficiency at a limited number of wavelengths (usually between 600 and 1000 nm) with lateral resolution. Würfel et al. [5] introduced another method to determine L_{eff} from electroluminescence images, restricting the detection to the short wavelength part of the luminescence spectrum.

It was proposed in Reference 6 that the collection diffusion length L_c could be obtained from electroluminescence images taken at near-bandgap wavelengths, since in this wavelength range the intensity of the luminescence emission is directly proportional to L_c. The aim of this paper is to review the theory behind this approach and to provide experimental evidence for the determination of L_c. For this purpose, we carry out electroluminescence measurements at near-bandgap wavelengths using an infrared-sensitive Indium-Gallium-Arsenide camera on a set of 15 specially prepared monocrystalline silicon solar cells with different thicknesses. The intensity of the electroluminescence emitted by these solar cells at near-bandgap wavelengths is shown to be proportional to the thickness, as expected from the physical model outlined below. Moreover, we demonstrate the applicability of the method introduced below to create images of the collection diffusion length of a multicrystalline silicon solar cell.

2. Modelling the electroluminescence emission at near-bandgap wavelengths

The electroluminescence (EL) photon flux Φ of wavelength λ emitted by a solar cell at a position (x_0, y_0) on the surface is described by the integral of the coefficient of radiative recombination B_{rad}, the electron and hole concentrations n and p and the probability of luminescence photon emission f_{em} over the thickness W of the solar cell [5,6]:

$$\Phi_{EL}(\lambda) = \int_0^W dz\, B_{rad}(\lambda)\, n(z)\, p(z)\, f_{em}(\lambda, z)\,. \qquad (1$$

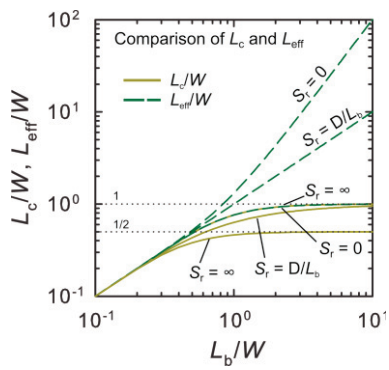

Figure 1. Dependence of the collection diffusion length L_c and the effective diffusion length L_{eff} on the bulk diffusion length L_b and the rear surface recombination velocity S_r. D is the diffusion constant.

For industrial solar cells, it is sufficient to consider only the contributions of the base region [7]. The photon emission probability f_{em} accounts for optical properties of the front and rear surface like reflectance and roughness as well as for photon reabsorption. Photon reabsorption is described by the Lambert-Beer law and depends on the wavelength λ and position z of the generated photon. For p-type solar cells (the following considerations hold analogously for n-type solar cells) at room temperature and under low level injection conditions, the hole concentration p is in good approximation equal to the doping concentration N_{dop} and thus independent of z [8]. B_{rad} is also in good approximation independent of z [9]. The electron concentration is obtained as a solution of the diffusion equation [8] and reads

$$n(z) \approx \frac{n_i^2}{N_{dop}} \exp\left(\frac{V}{V_T}\right) \tilde{n}(z) \tag{2}$$

where n_i is the intrinsic charge carrier concentration, V is the junction voltage, V_T is the thermal voltage and

$$\tilde{n}(z) = \cosh\left(\frac{L_b}{W}\right) - \frac{L_b}{L_{eff}} \sinh\left(\frac{L_b}{W}\right) \tag{3}$$

is the electron concentration normalized to its value at $z = 0$. In Eq. (3), L_b denotes the bulk diffusion length and L_{eff} the effective diffusion length

$$L_{eff} = L_b \frac{1 + S_r L_b / D \tanh(W / L_b)}{S_r L_b / D + \tanh(W / L_b)}. \tag{4}$$

D is the diffusion constant and S_r the rear surface recombination velocity. At near-bandgap wavelengths, where the absorption coefficient of silicon becomes very small [10], photon reabsorption is negligible and the emission probability f_{em} becomes independent of z. For industrial-type silicon solar cells, this approximation holds well for wavelengths above 1080 nm. This is visualized in Fig. 2, showing the ratio of the photon emission probability at $z = W$ to $z = 0$ calculated for a 200 µm thick planar sample. The integral in Eq. (1) then becomes equal to the collection diffusion length

$$\int_0^W dz\, \tilde{n}(z) = \frac{D L \sinh(W/L) + L^2 S\left[\cosh(W/L) - 1\right]}{L S \sinh(W/L) + D \cosh(W/L)} = L_c \tag{5}$$

as introduced by Brendel and Rau [2]. Consequently, the EL emission at near-bandgap wavelengths $\Phi_{EL,NBG}$ is proportional to L_c:

$$\Phi_{EL,NBG}(\lambda) = B_{rad}(\lambda)\, n_i^2 \exp\left(\frac{V}{V_T}\right) f_{em,NBG}(\lambda)\, L_c\,. \tag{6}$$

$f_{em,NBG}$ denotes the photon emission probability at near-bandgap wavelengths.

Often the luminescence emission is detected with a camera which provides spatial but not spectral resolution. At near-bandgap wavelengths, the number N_c of electrons per time generated in the detector by the incident photon flux $\Phi_{EL,NBG}$ is

$$N_c = \int_{1080\,nm}^{\infty} d\lambda\, \eta(\lambda)\, \Phi_{EL,NBG}(\lambda) = \text{const} \cdot L_c\,. \tag{7}$$

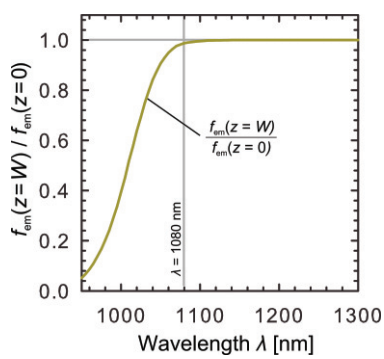

Figure 2. Ratio of the photon emission probability f_{em} at $z = W$ to $z = 0$ calculated for a 200 µm thick planar sample with a perfect mirror at the rear surface and neglectable reflectance of the front surface. For wavelengths above 1080 nm, $f_{em}(W)$ approaches $f_{em}(0)$. At these wavelengths, f_{em} is thus in good approximation independent of z.

$\eta(\lambda)$ contains the wavelength-dependent quantum efficiency of the detector and the conversion factor from generated electrons to detector signal. All other parameters have been subsumed into the proportionality factor. Consequently, the camera signal is also proportional to L_c.

3. Experimental test of the model

For solar cells with a rear surface recombination velocity $S_r \to \infty$ and a bulk diffusion length $L_b > 3W$, it follows from Eq. (3) that the minority carrier distribution decreases linearly from $z = 0$ to $z = W$, as shown in Fig. 3a. Since L_c is the integral of the normalized minority charge carrier concentration $\tilde{n}(z)$ over W, L_c is proportional to W in this case. Hence, according to the model given by Eq. (7), the camera signal should be proportional to W.

To confirm this prediction experimentally, we prepared a set of 15 monocrystalline silicon solar cells. Firstly, *p*-type 1,5 Ωcm FZ-silicon wafers with an area of 2×2 cm² were etched to obtain different thicknesses between 150 and 300 µm. The solar cells were then fabricated identically on these wafers and have an unpassivated and fully metallized rear surface, providing a very high rear surface recombination velocity S_r above 10^4 cm/s and a bulk diffusion length L_b of the minority charge carriers above 900 µm (corresponding to $L_b \geq 3W$). Both values have been confirmed by analyzing IQE measurements. These solar cells thus provide a good approximation to the idealized case of $S_r \to \infty$. The structure of the solar cells is shown schematically as an inlay in Fig. 3a.

EL measurements were carried out with the above described solar cells using an Indium-Gallium-Arsenide camera which is sensitive over the whole spectral range of EL emission. The applied voltage was 520 mV. An optical longpass filter with a cut-off wavelength of 1080 nm was mounted in front of the camera in order to restrict the detection to the long-wave luminescence emission. Our measurement setup is described in detail in Ref. 11. The global series resistance R_s was determined for each solar cell from a current-voltage characteristic and the corrected camera signal N_{corr} was obtained for each pixel by using the relation $N_{corr} = N_{meas} \cdot \exp(V_{Rs}/V_T)$ where N_{meas} is the measured camera signal and $V_{Rs} = j \cdot R_s$ is the voltage drop at the series resistance. It turned out that the impact of the series resistance on the camera signal is negligible. Each measurement was repeated 30 times to increase the signal-to-noise ratio. For the evaluation of the camera signal, values were averaged over 20 pixels between two fingers. Figure 3b shows the results of the measurements together with the model given by Eq. (7). The proportionality factor was determined using linear regression of the measured data.

The measured data is in good agreement with the model given in Eq. (7) and demonstrates that both the electroluminescence emission at near-bandgap wavelengths (i.e. wavelengths above 1080 nm) and the signal of the camera detecting the electroluminescence emission are proportional to the collection diffusion length L_c.

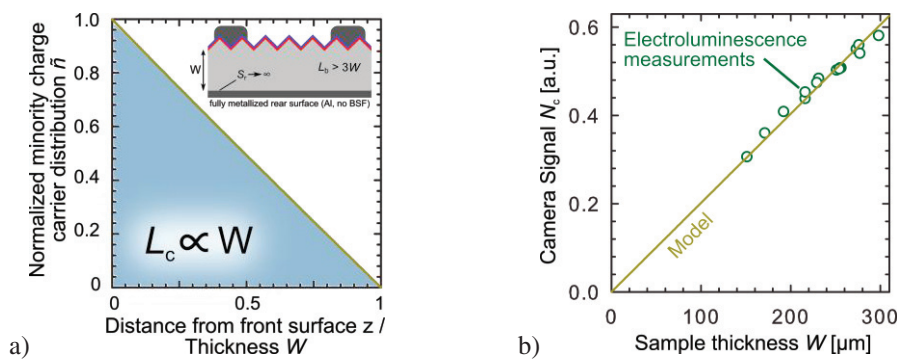

Figure 3. a) According to Eq. (3), the normalized minority charge carrier distribution decreases linearily from $z = 0$ to $z = W$ for the case of $L_b > 3W$ and $S_r \to \infty$. The inlay shows the structure of the solar cells discussed in section 3. b) The camera signal (circles) is proportional to the thickness of the sample, in accordance with the model given by Eq. (7) (solid line).

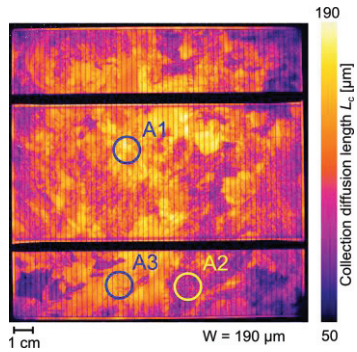

Figure 4. Mapping of the collection diffusion length L_c obtained by electroluminescence imaging using an infrared sensitive InGaAs camera equipped with a longpass filter with a cut-off wavelength of 1080 nm.

If the optical properties of the solar cell's surfaces are laterally homogenous, i.e. $f_{em,NBG}$ is not dependent on the lateral position (x_0, y_0) on the solar cell's surface, the proportionality factor in Eq. (7) is laterally constant and an EL image of the solar cell taken at near-bandgap wavelengths directly shows the collection diffusion length L_c in relative units [6]. This assumption usually holds for monocrystalline silicon solar cells with random pyramid textures or for iso-textured multicrystalline silicon solar cells, as investigated in this contribution. The proportionality factor can be determined by a calibration of the setup, e.g. by means of a local determination of L_c from an IQE measurement [1]. Alternatively, a calibrated spectrally resolved measurement of the emitted photon flux in absolute intensities could be performed. The first approach, which has already been demonstrated in Ref. 6, is evaluated in the following. For this purpose, Figure 4 shows an EL image of an iso-textured multicrystalline silicon solar cell. Again a longpass filter with a cut-off wavelength of 1080 nm was mounted in front of the detecting InGaAs camera in order to detect only the long-wave luminescence emission. The image was scaled using a locally determined value for L_c in the area A1 which was obtained from an IQE measurement. A realistic estimation of the accuracy of the determined L_c values yields 15 % relative. The total acquisition time for the EL image together with the additional IQE measurement is a few minutes.

To check consistency, local determinations of L_c were also carried out in the areas A2 and A3. Furthermore, the rear surface reflectance R_b and the lambertian factor Λ were determined from hemispherical reflectance measurements. The lambertian factor is a measure of the rear surface roughness [12]. $\Lambda = 0$ holds for a planar (i.e. specular reflecting) surface, $\Lambda = 1$ for a lambertian (i.e. diffuse reflecting) surface. Values inbetween describe a mixture of these idealized cases. Both R_b and Λ strongly affect the photon emission probability $f_{em,NBG}$ at near-bandgap wavelengths. Table 1 summarizes the determined values.

The image in Figure 4 visualizes the contribution of each area to the short circuit current of the solar cell when illuminated at near-bandgap wavelengths. Areas with a large collection diffusion length contribute significantly to the short circuit current. The collection diffusion length L_c determined in area A3 by a local IQE analysis agrees with the value taken from the scaled EL image with a relative deviation of 3 %. In area A2, a relative deviation between these two values of 13 % is found. As can be seen in Table 1, the difference of the optical parameters R_b and Λ between areas A1 and A2 is greater than between areas A1

Table 1. Collection diffusion length L_c, rear surface reflectance R_b and lambertian factor Λ in the areas A1-A3 in Fig. 4.

	Area A1	Area A2	Area A3
L_c [µm] from IQE measurement	180 ± 27	120 ± 18	158 ± 24
L_c [µm] from scaled image	-	105 ± 16	162 ± 24
Relative deviation	-	13 %	3 %
Lambertian factor Λ	0.48	0.66	0.55
Rear surface reflectance R_b	0.54	0.53	0.47

and A3, emphasizing the importance of laterally homogenous optical properties not only of the front surface but also of the rear surface if the image is scaled by a single factor.

4. Summary

The electroluminescence emission of silicon solar cells at near-bandgap wavelengths was modelled. It was shown that its intensity is directly proportional to the collection diffusion length L_c which is a function of the bulk diffusion length and the rear surface recombination velocity. Experimental evidence for the determination of L_c was provided by electroluminescence measurements carried out using an infrared sensitive Indium-Gallium-Arsenide camera on a set of 15 specially prepared solar cells of different thicknesses. For these solar cells, the emitted electroluminescence intensity at near-bandgap wavelengths is proportional to the thickness of the solar cell, in accordance with the model outlined in this contribution. Moreover, we demonstrated the applicability of L_c imaging with an industrial multicrystalline silicon solar cell and showed that lateral homogeneity of the optical properties of both the front and rear surface is required for this technique. For the sample investigated in this publication, the determined values for L_c coincide with values obtained from spectrally resolved quantum efficiency measurements with a relative accuracy of 13 %.

Acknowledgements

This work was supported by the scholarship program of the German Federal Environmental Foundation (Deutsche Bundesstiftung Umwelt).

References

[1] Basore P. Extended Spectral Analysis of Internal Quantum Efficiency. *Proc. 23rd IEEE Photovoltaic Specialists Conference, New York, USA*, 1993, p.147.
[2] Brendel R, Rau U. Injection and collection diffusion lengths of polycrystalline thin-film solar cells. *Sol. St. Phen.* 1999; **67-68**:81.
[3] Hirsch M, Rau U and Werner JH. Analysis of internal quantum efficiency and a new graphical evaluation scheme. *Solid State Electron.* 1995; **38**:1009.
[4] Warta W, Suttner J, Wagner BF and Schindler R. Impact of diffusion length distribution on the performance of mc-silicon solar cells. *Proc. 2nd World Conference on Photovoltaic Energy Conversion, Vienna, Austria*, 1998, p.1650.
[5] Würfel P, Trupke T and Puzzer T. Diffusion lenghts of silicon solar cells from luminescence images. *J. Appl. Phys.* 2007; **101**:123110.
[6] Bothe K, Hinken D, Ramspeck K, Fischer B and Brendel R. Combined Quantitative Analysis of Electroluminescence Images and LBIC Mappings. *Proc. 22nd European Photovoltaic Solar Energy Conference, Milan, Italy*, 2007, p.1673.
[7] Bothe K, Pohl P, Schmidt J, Weber T, Altermatt PP, Fischer B and Brendel R. Electroluminescence imaging as an in-line characterisation tool for solar cell production. *Proc. 21st European Photovoltaic Solar Energy Conference, Dresden, Germany*, 2006, p.597.
[8] Green MA. Solar Cells - Operating Priciples, Technology and System Application. University of New South Wales; 1992.
[9] Altermatt PP, Geelhaar F, Trupke T, Dai X, Neisser A and Daub E. Injection dependence of spontaneous radiative recombination in crystalline silicon: Experimental verification and theoretical analysis. *Appl. Phys. Lett.* 2006; **88**:261901.
[10] Green MA. Silicon Solar Cells - Advanced Priciples and Practice. University of New South Wales; 1995.
[11] Hinken D, Schinke C, Herlufsen S, Schmidt A, Bothe K and Brendel R. Experimental setup for camera-based measurements of electrically and optically stimulated luminescence of silicon solar cells and wafers, *Rev. Sci.Instrum.* 2011; **82**:033706.
[12] Brendel R, Hirsch M, Plieninger R and Werner JH. Quantum Efficiency Analysis of Thin-Layer Silicon Solar Cells with Back Surface Fields and Optical Confinement. *IEEE T. Electron Dev.* 1996; **43**:1104.